https://doi.org/10.5194/egusphere-2026-1847
Preprint. Discussion started: 2 April 2026

Brief Communication: Rise of the Guadalupe River- A Multifaceted Post Event Analysis of the July 4, 2025, Flood in Central Texas

Anupal Baruah[1], Dinuke Munasinghe[1], Sagy Cohen[1], Mohamed Abdelkader[2], Dipsikha Devi[1], Yixian Chen[1], Humberto Vergara[2]

[1]Department of Geography and Environment, University of Alabama, Tuscaloosa, USA
[2]IIHR—Hydroscience & Engineering, University of Iowa, Iowa, USA

Correspondence to: Anupal Baruah (abaruah@ua.edu), Sagy Cohen (sagy.cohen@ua.edu)

Abstract

The flash flooding across Central Texas on July 4th, 2025, caused more than 130 fatalities and property losses exceeding 20 billion dollars. The objective of this study is to diagnose the drivers of this catastrophic event and to analyze the temporal variability in forecasting flood inundation dynamics in the hours leading up to and during the event. Using the Operational National Water Model short-range streamflow forecast product, we generated 306 forecasted flood inundation maps between July 3rd and July 4th, 2025. For evaluation, we constructed an inundation extent benchmark derived from USGS high water marks. Both impact-based and pixel-based assessments are presented.

1. Introduction

On July 4th at dawn , a catastrophic flash flood hit Kerr and Kendall Counties in Texas, claiming at least 135 lives, making it one of the deadliest inland flooding events in United States history (https://psl.noaa.gov/news/2025/texasfloods.html). The event was triggered by intense rainfall up to 3-4 inches per hour in some of the impacted areas, causing flash flooding with exceptionally high peaks throughout the Guadalupe River basin. The Texas Hill Country, including Kerr and Kendall County, is prone to flash flooding, known as “Flash Flood Alley” (Saharia et al., 2017), partly due to the geomorphology of the area, having steep slopes and clay-rich soils, which result in high runoff rates (Sharif et al., 2010). Based on United States Geological Survey (USGS) streamflow observations, extreme flows were recorded downstream of the confluence of the South Fork Guadalupe River and the North Fork River (Figure 1d). At Hunt (Gage ID: 08615500), the streamflow reached 8,260.8 m^3/s at 5:05 AM, far exceeding the 500-year return period flow of 4,160.8 m^3/s. A significant portion of this peak was contributed by the ungauged South Fork

https://doi.org/10.5194/egusphere-2026-1847
Preprint. Discussion started: 2 April 2026

Guadalupe River, which caused numerous fatalities near Camp Mystic (Nevitt 2025). Further downstream, at Kerrville, the streamflow peaked at 8,316.0 m^3/s at 6:45 AM, crossing the 500-year return period flow of 7,937.6 m^3/s. Apart from the peak values, the hydrographs at both upstream gauge stations exhibited exceptionally short times to peak, reaching the 500-year return period level within just 1–1.5 hours. This rapid rise of flow is indicative of extremely high runoff response, amplifying the severity of the event.

The main motivation of this study was to utilize multiple operational forecast Flood Inundation Maps (FIM) and conduct an extensive impact-based and categorical assessment of the event across different forecast hours against high water mark derived benchmark FIM. We employed the National Weather Service (NWS) National Water Model (NWM) short-range forecast and the FIMserv tool (Baruah et al., 2025) to generate 306 FIMs at the Hydrologic Unit Code (HUC)-8 scale. Additionally, we developed a methodology to use post-event USGS observed high-water marks to create a spatially continuous FIM benchmark for evaluating the forecast FIMs. Our objective is to investigate the trade-off between NWM forecast range and the reliability of flood impact predictions. Specifically, we examined how FIM forecast skill, including building-level impacts, varied with respect to different forecast hours at five different locations (four streamflow gauges and near Camp Mystic).

2. Hydrometeorological Assessment

Between July 3rd and 6th, 2025, the Texas Hill County region experienced an extraordinary rainfall amounts that produced catastrophic flash flooding along the Guadalupe River (Figure 1a-1c). The event was initiated by remnant moisture from Tropical Storm Barry, which had made landfall in Mexico days earlier, and was further intensified by a mesoscale convective vortex embedded within a persistent mid-level trough. These factors, combined with a strengthening low-level jet to sustain widespread convection, favor back-building successive thunderstorms across the Hill County (WPC, 2025). Hourly precipitation amounts from the Multi-Radar Multi-Sensor (MRMS) gauge-corrected quantitative precipitation estimation (QPE) dataset (Zhang et al., 2016), supplemented with rain gauge observations, reveal accumulations exceeding 500 mm (20 inch) in parts of the upper Guadalupe basin between July 3 to July 6 (Figure 1b). Rainfall intensities surpassed 100-year return period thresholds for durations ranging from 3 to 24 hours at the rainfall

https://doi.org/10.5194/egusphere-2026-1847
Preprint. Discussion started: 2 April 2026

gauges when compared against NOAA Atlas 14 precipitation frequency curves (Perica et al., 2018; NSSL, 2025). One of the most severe bursts occurred between 2 AM and 5 AM on July 4, when localized rainfall rates reached 100 mm/h (Figure 1e, Figure S2). The persistence of convective regeneration amplified accumulations and produced rainfall totals approaching 460 mm in some localized areas on July 4. Gauge records showed peaks at stations in the western part of the basin that aligned with MRMS QPE observations, where total precipitation indicated higher accumulations (Figure 1b, e, Figure S2).

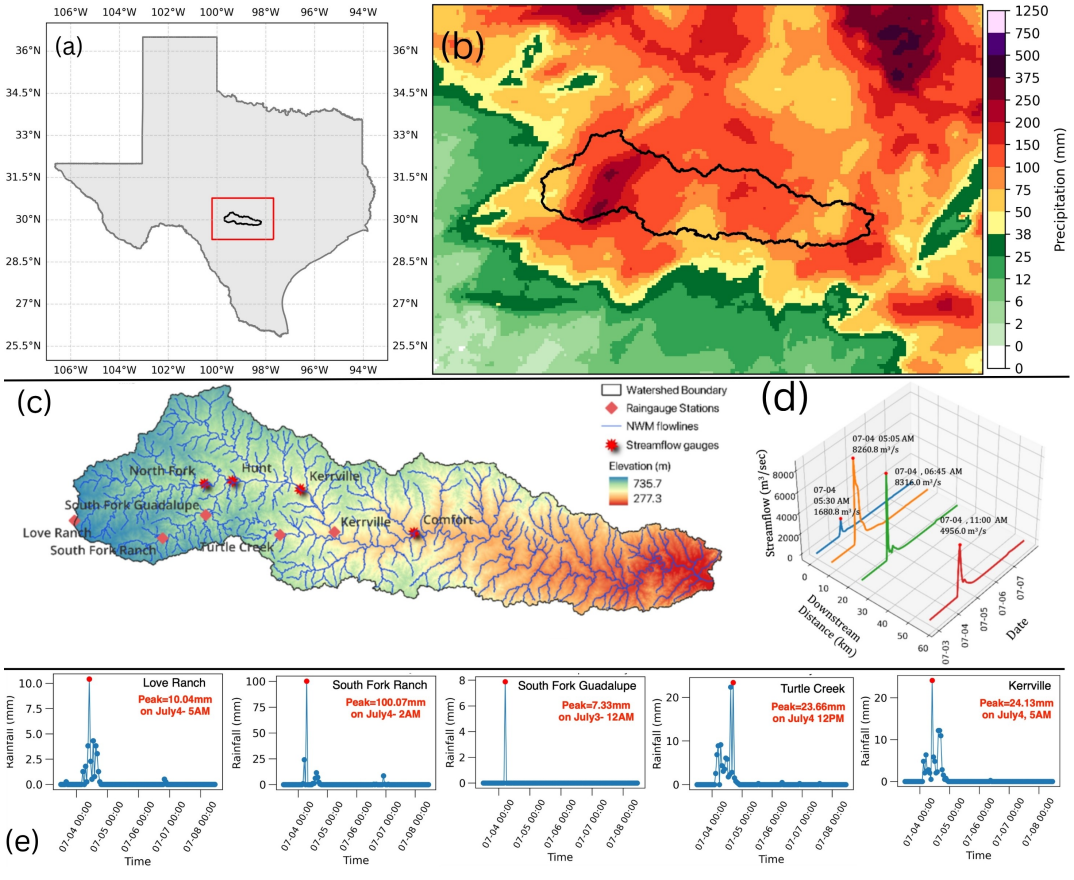

https://doi.org/10.5194/egusphere-2026-1847
Preprint. Discussion started: 2 April 2026

Figure 1. (a) Geographical location of the study area, (b) MRMS-derived total precipitation between 4–6 July 2025, (c) locations of USGS streamflow and rainfall gauges, (d) Gauge streamflow records along the reach, and (e) hourly rainfall time series.

The NWM short-range forecasts (SRF) provide hourly streamflow predictions extending to 18 hours forecast range (https://water.noaa.gov/about/nwm). We identified the NWM flowlines (feature_id) that intersect with the USGS gages and downloaded the SRF generated (Figure 2) from 10 PM, July 3rd till 2 PM, July 4th using FIMserv. At North Fork (peak at 5.30 AM), earlier SRFs show no flooding conditions, but there is a sudden jump on the forecast generated on July 4 , between 4 AM to 7AM (120 m^3/sec to 600 m^3/sec). At Hunt (peak at 5:05 AM), the forecast generated for 4 AM indicates a possibility that flow will cross 500 m^3/sec (above 2 Year RP flow of 266.08 m^3/sec) in the next two hours, while the forecast generated for 5 AM, reaches the 10-year RP (1276.52 m^3/sec). Further downstream, at Kerrville (peak at 6:45 AM), there was no indication of a high flow event; however, the forecast generated for 6 AM shows that flow will exceed the 2-year return period flow (284.22 m^3/sec). At Comfort (peak at 11:00 AM), the initial forecast shows low flows, while the forecast generated after 10 AM indicates that flow will exceed the 10-year RP flow (1842.73 m^3/sec), and the subsequent forecast follows the same trend. Near Camp Mystic, for which we do not have a USGS gage, the forecast for 4 AM in South Fork Guadalupe River predicted a peak of 750 m^3/sec. A Zoom-in view of the generated forecast closer to the event is shown in Figure-S1 of the supplementary material.

https://doi.org/10.5194/egusphere-2026-1847
Preprint. Discussion started: 2 April 2026

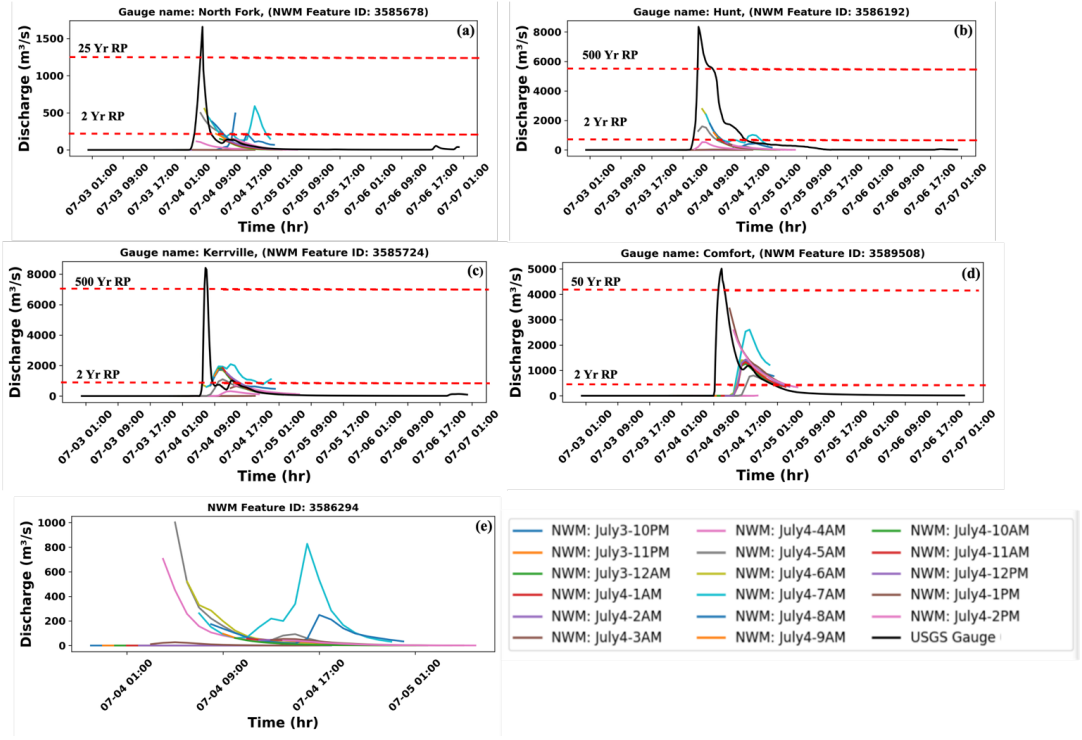

Figure 2. NWM short-range forecast at different lead times at (a) North Fork (b) Hunt (c) Kerrville (d) Comfort and (e) Camp Mystic. The red dash line indicates the return period flow exceeded by the gage readings.

Overall, the NWM SRF deviated substantially from the USGS observations in this case (Figure 2). These underpredictions in NWM SRF during the flood event were strongly affected by two primary sources of uncertainty: 1) Inconsistency in the location and magnitude of precipitation rates in the precipitation forcing from the High-Resolution Rapid Refresh (HRRR) model leading up to the event, and ii) the failure of USGS stream gauges used for data assimilation. The NWM short-range configuration relies on HRRR Quantitative Precipitation Forecast (QPF) at 3-km resolution to drive runoff generation (Dowel et al., 2022). A rainfall-to-rainfall comparison between the HRRR-QPF and MRMS Quantitative Precipitation Estimate (QPE) indicated a notable underestimation in the HRRR rainfall forecasts (Figure S3 in the supplementary material). When QPF underestimates or spatially misplaces convective rainfall cells, the resulting simulated discharge and flood peaks are either lower in magnitude or displaced in time relative to observations (Krajewski et al., 2025; Vergara et al., 2023). This bias has a pronounced effect on

https://doi.org/10.5194/egusphere-2026-1847
Preprint. Discussion started: 2 April 2026

streamflow forecasts, especially for basins smaller than 1,000 km² that are prone to flash flooding (Krajewski et al., 2025). The combination of the spatially misplaced QPF, smaller basin sizes, and flash flood prone geomorphology caused the NWM to signal intense flooding potential in the basins surrounding the Guadalupe River in the hours leading up to the event. However, the changing signal location in each timestep resulted in underprediction for the Guadalupe basin. The underestimation in the NWM during the event was exacerbated by the failure of the USGS gauge 08165500 near Hunt on the Guadalupe River during the fast-rising streamflow, as seen from the outage of data on the USGS water data gauge page from July 4th to the 5th (https://wik.ly/3Wjb6hk). This outage disrupted the NWM's data assimilation process (Seo et al., 2021) from performing streamflow "nudging" to correct model states toward observed discharge. These errors were extrapolated with downstream flow propagation, resulting in systematic underprediction of streamflow.

3. Forecast FIM Generation and Evaluation

We used FIMserv to generate 306 flood inundation maps using the above described NWM forecasted flows. FIMserv assigns each forecast as an inflow to the OWP HAND-FIM model, which uses reach-averaged synthetic rating curves to generate binary FIMs, based on the Height Above Nearest Drainage (HAND) approach (Aristizabal et al., 2023; Chen et al.,2025).

3.1 Derivation of Maximum Forecasted Inundation

The maximum extents from the forecast FIMs at a given reference time are estimated by combining multiple short-range forecast FIMs (Figure S4 in the supplementary material). For example, to assess flooding on July 4th, 5:00 am (reference time), we used the maximum inundation extent from a total of 7 forecasts from earlier timestamps (10 pm July 3 through 4:00 am July 4) that predict conditions at 5:00 am. Each raster (i.e., each of the 7 forecasts) was stacked, and for each pixel, if it was marked as flooded in any raster, it was considered flooded in the final composite. This approach produces a temporally integrated, conservative estimate of potential flooding (i.e., the largest possible forecasted extent for that hour), capturing uncertainty and variability in subsequent short-range forecasts.

3.2 Flood benchmark map creation using High Water Marks (HWMs)

https://doi.org/10.5194/egusphere-2026-1847
Preprint. Discussion started: 2 April 2026

We used the USGS High-water marks (HWMs) as the primary reference data for the creation of the benchmark FIM. HWM observations were obtained from the USGS Short-Term Network (STN) database (https://stn.wim.usgs.gov/STNDataPortal/#) and subjected to multi-stage preprocessing. First HWMs were filtered based on data quality ("Good" or "Excellent" quality were retained). Surveyed elevations (elev_ft) were converted to metric units (elev_m) relative to mean sea level. Next, global outlier removal was performed using the interquartile range (IQR) method (Tukey, 1977) to eliminate extreme data points. Subsequently, spatial outliers were identified using Local Moran's I, which evaluates each HWM in the context of its neighboring points rather than the dataset as a whole. The spatial relationships are defined using a weights matrix, with the neighborhood distance empirically determined through semivariogram analysis. This approach ensures that the detection of local outliers reflects the natural decay of spatial autocorrelation across the floodplain, improving the reliability of the interpolated water surface elevation. The filtered HWM dataset was then interpolated into a continuous Water Surface Elevation (WSE) raster using the Topo to Raster algorithm in ArcGIS Pro 3.4.0, a hydrologically conditioned interpolation approach that enforces drainage continuity (Feaster and Koeing.,2017; Koeing et al., 2016). The interpolated WSE surface was subtracted from a 10 m Digital Elevation Model (DEM), yielding flood depth estimates. Cells with positive residuals (DEM ≤ WSE) were classified as inundated, while negative residuals were assigned as non-flooded. This procedure yielded a benchmark flood inundation map derived solely from empirical HWM data that was used in FIM forecast evaluations in subsequent sections.

3.3 Evaluation of the forecasted FIM against the benchmark FIM

We used FIMeval (Devi et al., 2025) to evaluate the forecasted FIMs at five locations (Figure 3) across different forecast times against the benchmark FIM. Since the HWM-derived benchmark is static (maximum inundation) and the exact time at which the HWMs were attained during the flood event is unknown, the gage-recorded peak time was used as the reference, and forecasted FIMs were evaluated within a ±2-hour window around this reference hour. This introduces an additional source of temporal uncertainty into the overall evaluation process. For pixel-based assessment, we used Critical Success Index (CSI), F1-Score, Probability of Detection (POD), and False Alarm Rate (FAR) as the evaluation matrix (Figure 3), and for impact assessment, we compared the number of predicted and observed flooded buildings at different forecast times.

https://doi.org/10.5194/egusphere-2026-1847
Preprint. Discussion started: 2 April 2026

At North Fork, the flood peak occurred at 5:30 AM. Compared to earlier forecasts, the FIM forecasts for 4 AM to 6 AM show gradual improvements in CSI, F1, and POD scores, although the 4 AM forecast also exhibits a higher FAR (Figure 3a1). The impact assessment (Figures 3a2–a5) indicates that 4 AM forecast FIM predicts no building flooded, 5 AM forecast predicts two flooded buildings, whereas the benchmark FIM shows 13 flooded buildings. Near Camp Mystic, the evaluation scores for the 4 and 5 AM forecasts improved substantially compared to earlier forecasts (Figure 3b1). In terms of impacts, the benchmark FIM shows 118 buildings affected, while the 4 AM and 5 AM forecasts predict only 18 and 72 flooded buildings, respectively (Figures 3b2–b6). At Hunt, the flood peak was recorded at 5:05 AM. Here, the evaluation scores also improved, with CSI values increasing from 0.34 for the 4 AM forecast to 0.52 for the 5 AM forecast, while earlier forecasts yielded much lower scores (<0.25) (Figure 3c1). The impact assessment (Figures 3c2–c6) indicates that the benchmark FIM estimates 133 buildings impacted, compared to only 19 for the 5 AM forecast and only 2 for the 4 AM forecast. At Kerr, the peak was recorded at 6:45 AM. Here, we found higher evaluation scores in the post-event forecast. For instance, the CSI scores are below 0.30 for 6 AM, but the scores are increasing at 10 AM, at 0.53. A similar trend was observed in POD and F1 score. From the impact assessment, we found that the benchmark FIM shows 140 flooded buildings, while the forecast FIMs have only one building flooded at 6 AM. We also observed notable underprediction in forecast FIM extents downstream of hydraulic structures (Figure 3d2-d4). Such discrepancies likely stem from artifacts in the HAND raster and insufficient representation of dam release flows in the NWM streamflow forecasts (Aristizabal et al., 2023; Kim et al., 2020). At Comfort, the flood peak occurred at 11:00 AM. Early forecasts showed very low scores (<0.1), but the scores improved at 1 PM (Figure 3e1). Eventually, we found no buildings hit from the predicted FIMs until 1 PM, while the benchmark indicates 188 flooded buildings (Figure 3 e2-e6).

https://doi.org/10.5194/egusphere-2026-1847
Preprint. Discussion started: 2 April 2026

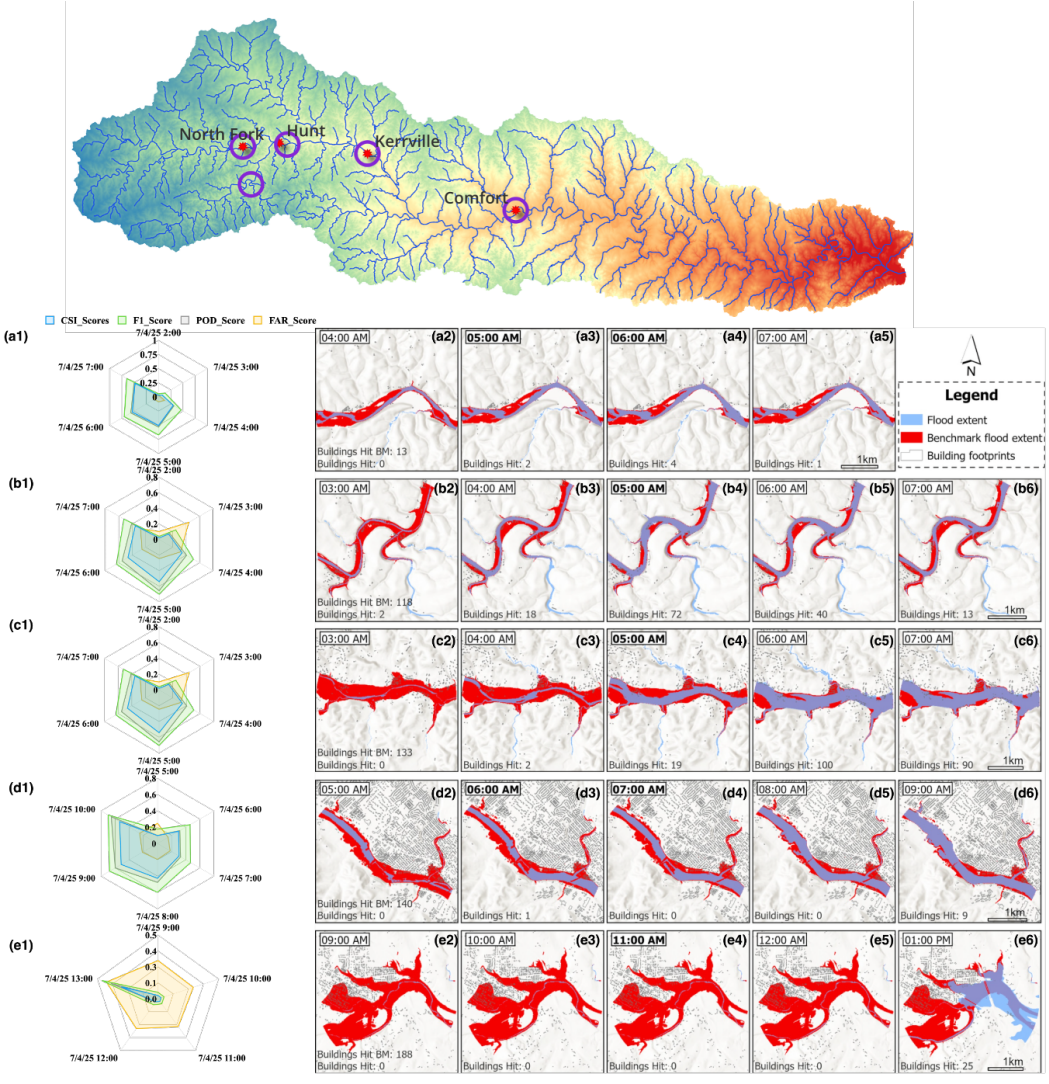

Figure 3. Top panel shows the FIM evaluation extent. (a) North Fork (b) Camp Mystic (c) Hunt (d) Kerr and (e) Comfort. The bottom left panel (a1-e1) shows the accuracy metrics of FIM evaluation and the right panel (a2-e6) shows the forecast flood extent, benchmark flood extent, and number of building hits at different forecast hours. Each subpanel lists the forecast hour in the upper-left box; times that coincide with, or cover, the USGS-observed peak discharge are highlighted in bold.

https://doi.org/10.5194/egusphere-2026-1847
Preprint. Discussion started: 2 April 2026

4. Closing Remarks

In this brief communication, we highlight the hydroclimatic drivers and impacts of the Texas flash flood event on July 4, 2025. Using USGS gauge observations, we analyzed the NWM short-range streamflow forecasts. Across all four-gauge locations, the NWM short-range forecasts considerably underpredicted the peak flow, with a pronounced lag between observed and forecasted flows at downstream sites. We found that underprediction and lag in short range forecasts are mainly due to the errors in rainfall estimation and the failure of data assimilation ("nudging") caused by malfunctioning USGS gauges during the peak flow. These streamflow underpredictions seem to have propagated, resulting in substantially underestimated flood extents in forecasted FIMs at different lead times. Using the gauge-recorded peak time as a reference, we evaluated forecast FIMs at different hours. against a benchmark flood inundation extent generated using ground-sampled high-water marks from USGS. At upstream gages, forecast skill improved as the forecast time approached the reference peak, whereas at downstream locations (Kerr and Comfort), evaluation scores were very poor at the reference time but improved after the observed peak flow. It is also clear from the impact assessment that forecast FIM was unable to capture the majority of flooded buildings compared to the benchmark. This case study points to the need for communicating the uncertainty and error bounds in operational forecast FIMs for early response and decision-making. One promising approach is probabilistic FIM which can effectively represent and leverage uncertainty in streamflow forecasts, providing more informative and actionable guidance for emergency responders.

Code and data availability

Code for downloading the NWM short-range forecast and for producing the flood inundation maps is available at https://github.com/sdmlua/FIMserv. The benchmark high water flood inundation map for the Texas Flood event is available in https://github.com/sdmlua/fimbench

Author contributions

Conceptualization: Anupal Baruah, Dinuke Munasinghe, Sagy Cohen. Formal analysis and methodology: Anupal Baruah, Dinuke Munasinghe, Mohamed Abdelkader, Dipsikha Devi, Yixian Chen, Derek Supervision: Sagy Cohen. Writing (original draft preparation): Anupal

https://doi.org/10.5194/egusphere-2026-1847
Preprint. Discussion started: 2 April 2026

Baruah, Mohamed Abdelkader, Dinuke Munasinghe, Dipsikha Devi, Riley McDermott, Derek Giardino, Humberto Vergara. All authors reviewed the final paper.

Acknowledgments

Funding for this project was provided by the National Oceanic & Atmospheric Administration (NOAA), awarded to the Cooperative Institute for Research to Operations in Hydrology (CIROH) through the Cooperative Agreement with The University of Alabama (NA22NWS4320003).

Conflict of Interest

None of the authors has any conflict of interests

Disclaimer

The scientific results and conclusions, as well as any views or opinions expressed herein, are those of the authors and do not necessarily reflect the views of NOAA.

References

1. Aristizabal, F., Salas, F., Petrochenkov, G., Grout, T., Avant, B., Bates, B., ... & Judge, J. (2023). Extending height above nearest drainage to model multiple fluvial sources in flood inundation mapping applications for the US National Water Model. Water resources research, 59(5), e2022WR032039.
2. Baruah, A., Dhital, S., Cohen, S., Tran, T. N. D., Elhaddad, H., Watts, C. L., Devi ,D., Chen, Y., & Pruitt, C. (2025). FIMserv v. 1.0: A tool for streamlining Flood Inundation Mapping (FIM) using the United States operational hydrological forecasting framework. Environmental Modelling & Software, 106581.
3. Chen, Y., Cohen, S., Baruah, A. *et al.* Merging Remote Sensing Derived River Slope Datasets with High-Resolution Hydrofabrics for the United States. *Sci Data* **12**, 1657 (2025). https://doi.org/10.1038/s41597-025-05941-6
4. Devi, D., Dhital, S., Munasinghe, D., Baruah, A., Chen, Y., Tian, D., & Pruitt, C. (2026). A framework for the evaluation of flood inundation predictions over extensive benchmark databases. Environmental Modelling & Software, 196, 106786. https://doi.org/10.1016/j.envsoft.2025.106786
5. Dowell, D. C., Alexander, C. R., James, E. P., Weygandt, S. S., Benjamin, S. G., Manikin, G. S., & Alcott, T. I. (2022). The High-Resolution Rapid Refresh (HRRR): An hourly updating convection-allowing forecast model. Part I: Motivation and system description. Weather and Forecasting, 37(8), 1371-1395.

https://doi.org/10.5194/egusphere-2026-1847
Preprint. Discussion started: 2 April 2026

6. Feaster, T. D., & Koenig, T. A. (2017). Field manual for identifying and preserving high-water mark data (No. 2017-1105). US Geological Survey.
7. July 2025 Central Texas floods. (n.d.). In Wikipedia. Retrieved January 12, 2026, https://en.wikipedia.org/wiki/July_2025_Central_Texas_floods
8. Kim, J., Read, L., Johnson, L. E., Gochis, D., Cifelli, R., & Han, H. (2020). An experiment on reservoir representation schemes to improve hydrologic prediction: Coupling the national water model with the HEC-ResSim. Hydrological Sciences Journal, 65(10), 1652-1666
9. Krajewski, W. F. (2025). Is this rainfall forecast good or bad? For flood forecasting, the answer is scale-dependent. Bulletin of the American Meteorological Society, 106(9). https://doi.org/10.1175/BAMS-D-24-0166.1
10. Koenig, T. A., Bruce, J. L., O'Connor, J., McGee, B. D., Holmes Jr, R. R., Hollins, R., ... & Peppler, M. C. (2016). Identifying and preserving high-water mark data (No. 3-A24). US Geological Survey.
11. Musser, J. W., Watson, K. M., Painter, J. A., & Gotvald, A. J. (2016). Flood-inundation maps of selected areas affected by the flood of October 2015 in central and coastal South Carolina (No. 2016-1019). US Geological Survey.
12. National Research Council (NRC). (2009). Mapping the Zone: Improving Flood Map Accuracy. National Academies Press.
13. Saharia, M., Kirstetter, P.-E., Vergara, H., Gourley, J. J., Hong, Y., & Giroud, M. (2017). Mapping flash flood severity in the United States. Journal of Hydrometeorology, 18(2), 397–411
14. Seo, B. C., Krajewski, W. F., & Quintero, F. (2021). Multi-scale hydrologic evaluation of the national water model streamflow data assimilation. JAWRA Journal of the American Water Resources Association, 57(6), 875-884.
15. Sharif, H. O., Hunter, N. M., & Wang, Q. J. (2010). Hydrologic modeling of an extreme flood event using distributed physically-based models. Journal of the American Water Resources Association, 46(2), 292–307. https://doi.org/10.1111/j.1752-1688.2010.00459.x
16. Vergara, H., Gourley, J. J., & Erickson, M. (2023). An efficient ensemble technique for hydrologic forecasting driven by quantitative precipitation forecasts. Journal of Hydrometeorology, 24(3), 479–495. https://doi.org/10.1175/JHM-D-22-0109.1
17. Watson, K. M., Storm, J. B., Breaker, B. K., & Rose, C. E. (2017). Characterization of peak streamflows and flood inundation of selected areas in Louisiana from the August 2016 flood (No. 2017-5005). US Geological Survey.
18. Weather Prediction Center (WPC), Mesoscale Precipitation Discussion: #0582, https://www.wpc.ncep.noaa.gov/metwatch/metwatch_mpd_multi.php?md=582&yr=2025
19. Zhang, J., Howard, K., Langston, C., Kaney, B., Qi, Y., Tang, L., ... & Kitzmiller, D. (2016). Multi-Radar Multi-Sensor (MRMS) quantitative precipitation estimation: Initial operating capabilities. Bulletin of the American Meteorological Society, 97(4), 621-638.

https://doi.org/10.5194/egusphere-2026-1847
Preprint. Discussion started: 2 April 2026

295 20. National Severe Storms Laboratory, Multi-Radar Multi-Sensor Operational Product
296 Viewer, https://mrms.nssl.noaa.gov/qvs/product_viewer/.

297